Kinetic Perimetry on Virtual Reality Headset

Rossana Terracciano, Alice Mascolo, Laura Venturo, Federica Guidi, Mariangela Vaira, Chiara M. Eandi and Danilo Demarchi, *Senior Member*, IEEE

***Abstract*— *Objective*: We present a portable automatic kinetic perimeter based on a virtual reality (VR) headset device as an innovative and alternative solution for the screening of clinical visual fields. We compared the performances of our solution with a gold standard perimeter, validating the test on healthy subjects. Methods: The system is composed of an Oculus Quest 2 VR headset with a clicker for participant response feedback. An Android app was designed in Unity to generate moving stimuli along vectors, following a standard Goldmann kinetic perimetry approach. Sensitivity thresholds are obtained by moving centripetally three different targets (V/4e, IV/1e, III/1e) along 24 or 12 vectors from an area of non-seeing to an area of seeing and then transmitted wirelessly to a PC. A Python real-time algorithm processes the incoming kinetic results and displays the hill of vision in a two-dimensional map (isopter). We involved 21 subjects (5 males and 16 females, age range 22–73 years) for a total of 42 eyes tested with our proposed solution, and results were compared with a Humphrey visual field analyzer to test reproducibility and efficacy. Results: isopters generated with the Oculus headset were in good agreement with those acquired with a commercial device (Pearson's correlation values r > 0.83 for each target). Conclusions: we demonstrate the feasibility of VR kinetic perimetry by comparing performances between our system and a clinically used perimeter in healthy subjects. Significance: proposed device leads the way for a portable and more accessible visual field test, overcoming challenges in current kinetic perimetry practices.**

***Index Terms*— Kinetic Visual Field, VR, Wearable, Portable Medical Devices, Ophthalmology**

I. Introduction

VISUAL field test is a clinical examination that measures the light sensitivity of the human retina in central and peripheral areas of the visual field, determining and often localizing vision loss to a specific anatomic location [1], [2]. The visual field test has played an essential role in early diagnosis and management of various medical conditions that damage vision gradually such as glaucoma [3], [4], pituitary adenoma [5], brain tumors [5], strokes [6], and several neurological conditions [7], [8].

R. Terracciano, A. Mascolo and D. Demarchi are with the Department of Electronics and Telecommunications, Politecnico di Torino - Torino, Italy. L. Venturo, F. Guidi, M. Vaira, C. M. Eandi are with School of Orthoptic, Department of Surgical Sciences, University of Torino, Torino, Italy.

To date, there are mainly two methods used in clinical settings to evaluate the visual field: static and kinetic perimetry. In static perimetry, a bright stimulus is presented in a specific test point location of the visual field while its luminance is changed gradually until it is seen [9]. In kinetic perimetry, instead, the bright stimulus is dynamically moved along a specific path of the visual field while target size and luminance are fixed [10]. While static perimetry is normally used to evaluate the central field (within 30°) [11] and the testing duration is relatively short (10-25 min for a bilateral examination, depending on the perimetrist's skills) [12], [13], kinetic perimetry measures both central and peripheral areas of the visual field and it is more sensitive to advanced visual field loss and edge detection of such defects [14], [15], allowing to accurately characterize the shape of visual field deficits. Among kinetic perimetry techniques, Goldmann kinetic perimetry is considered the gold standard test for assessing the peripheral visual field. Although this method is performed manually [16], it lacks standardization since it is technician-dependent [17], it requires intensive training of the clinicians performing the examination as well as patient collaboration, and parameters such as fatigue, learning effect, artifacts or measurement errors contribute to the variability of the test [18], [19]. Despite automatic kinetic has been introduced to increase standardization, issues to be addressed include examiner bias which generates large individual differences in clinical performance among examiners and poor comparability between results obtained from different clinics [13], [20], intra-examiner differences in choosing stimulus velocity [21], as well as limited normative population characteristics [22], and longer duration of the automated test compared to the standard Goldmann perimetry (up to 50 minutes for a bilateral examination) [23]. Another limitation of kinetic perimetry instruments is that these machines are large and immobile, and they are confined in a single location which makes the exam restricted to only collaborative patients who can keep a prolonged standing posture while excluding all the patients with reduced cervical flexibility and postural reactivity [24], [25], as well as patients with other range-limiting conditions [26].

Therefore, portable solutions for visual field examinations which can be used at the bedside can significantly improve clinical outcomes translating to patients unable to fully sit up. In this regard, virtual reality (VR) goggles or headsets have recently shown promising benefits as potential ophthalmologic diagnostic devices [27]–[29], including an increase in patient comfort associated with a decrease in test-induced fatigue which makes them suitable even for patients affected with

restrictive neck conditions [30], and the possibility to expand the option of remote testing. In addition, the diagnostic utility of VR has been demonstrated to address current challenges associated with inattention and poor compliance for the detection of visual field defects in children [31]. Tsapakis et al. [32], [33] presented a visual field examination method using virtual reality glasses which implements static perimetry and evaluated the reliability of the method in glaucoma patients by comparing the results with those of a standard perimeter obtaining promising correlation results. Other examples of commercially available perimeters are the VisuALL which utilizes a game-based format to engage the attention of children [26], as well as Advanced Vision Analyzer (AVA; Elisar Vision Technology) [34], and the head-mounted automated perimeter imo® [35], [36] which have both proven efficacy in the diagnosis of glaucoma. Kunumpol et al. [37] presented in a conference paper a system known as the GlauCUTU Visual Field test that utilizes a portable VR headset with visual stimulus that progressively increases in intensity and tested this device comparing a control group of normal fields and subjects with glaucoma, demonstrating the translational value of GlauCUTU. However, these previously reported studies involve only static perimetry, limiting the examination to the central field, and still limited data confirm their validity [38].

To our knowledge, there is no previous study reporting VR headsets implementing kinetic perimetry. Therefore, we present here for the first time a portable automatic kinetic perimeter based on a VR headset device as an innovative and alternative solution for the visual field clinical examination. In this study, the visual field was examined with three different isopters with 24 (for the V/4e) or 12 stimuli (for the IV/1e and III/1e) presentations per isopter and sent wirelessly to the physician PC. With our kinetic perimetry system, patients do not require to maintain a particular head position as the headset adjusts to the patient's head movements. In addition, the field analyzer reduces overall testing time keeping the binocular vision. We tested our solution on 21 subjects, and we compared our protocol with a commercial perimeter (Humphrey HFA 3, Zeiss®). The main contribution of this paper is the implementation of a portable perimeter device that leads the way for a more accessible visual field test, overcoming challenges in current kinetic perimetry practices.

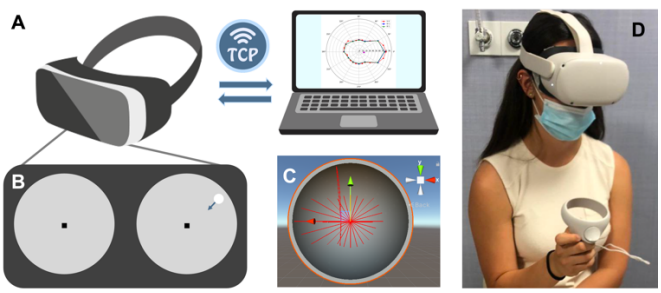

Figure 1. Portable automatic kinetic perimeter based on a virtual reality device: experimental setup. (A) schematic representing the Oculus Quest 2 headset which exchanges data with a Python client through TCP protocol; (B) binocular view within the headset; (C) Frontal view of the testing dome in Unity with vector trajectories indicated in red; (D) Representative photo of the headset while the kinetic perimetry test was running for one of the subjects involved in the study.

II. Methods

A. Instrumentation

All kinetic perimetry tests reported in this study were performed at the School of Orthoptic, Department of Surgical Sciences, University of Torino, Italy. Oculus VR kinetic perimetry system was compared to a clinically and routinely used perimeter on healthy subjects using a Humphrey Field Analyzer 3 perimeter (ZEISS, Oberkochen, Germany). The testing protocol and setting parameters were conformed to both devices and detailed described in Subsection B (Data Acquisition).

A schematic of the kinetic system proposed in this study is represented in Figure 1. It contains a virtual reality headset that generates the visual field test, the Bluetooth-connected clicker to generate the subject feedback, and a laptop computer with a Graphical User Interface (GUI) which receive wirelessly the data and plot the bidimensional maps representing the field of view. To simulate a standard kinetic visual field, our VR system uses the commercially available Oculus Quest 2 VR headset. To implement the same testing principles as in the Humphrey we used Unity 2020.3.24f1. A Goldmann bowl with a radius of 30 cm, was created in VR while each stimulus was presented moving radially from the periphery of the bowl toward the center following a vector (Fig.1B). A fixation point was placed in the center of the bowl. The start and end points for each vector were predefined to produce shorter examination durations, starting at the outer border region of the normal visual field (Fig.1C). To normalize the stimulus size and intensity, we used the manual Goldmann kinetic perimeter conventions, where size V corresponds to 64 mm^2, size IV corresponds to 16 mm^2, and size III corresponds to 4 mm^2, while Goldmann stimulus intensities are presented in 1 dB steps from the darkest 1a to the brightest 4e intensity. Following these indications, we generated three peripheral isopters, consisting of 24 vectors for the V/4e ispopter (every 15° meridian), while the innermost isopters (IV/1e and III/1e) consisted of 12 vectors (every 15° meridian). Each vector of an isopter was presented to the subject in random order while keeping the progressive order V/4e, IV/1e, and III/1e (varying the size and intensity of the stimuli from more visible to less visible) for all the subjects. Visual stimuli moved along 24 or 12 vectors randomly at a constant angular velocity of 5 °/s. A physiologic scotoma (blind spot, corresponding to the optic disc and devoid of photoreceptors) is localized using 4 centrifugal vectors, 15° temporally at a constant angular velocity of 2 °/s, starting from the point identified by the standard anatomical coordinates of the optic disc. The background luminance of the bowl was 31.5 apostilbs (10 cd/m^2). Luminance test parameters (background illumination and stimulus characteristics) were identical to those applied in the Humphrey kinetic perimetry and measured in both instruments using a photometer (Testo 540,

TEquipment, Long Branch, NJ, USA, Part Number: 05600540). On the other side, a Python GUI collects the patient feedback and the radius of each vector seen in his field of view and update in real-time the bidimensional map while saving and storing patient data into an Excel file. Data exchange and communication occur wirelessly, using TCP IP communication protocol. GUI was realized using Tkinter, while Pandas, Numpy and Matplotlib were used to plot, save, and store the data.

B. Data Acquisition

Humphrey visual fields were tested in monocular vision, using a monocular on both eyes of each subject. Oculus visual fields were tested in binocular vision, but single-eye measurement was performed. Indeed, the target was presented only for one eye per time while the examinee's view was maintained binocular, as shown in a schematic in Figure 1B following the approach by Kimura et al. [35]. For instance, when the right eye is tested and vision remains binocular, the stimulus is presented only in the right display. In this way, the subject does not perceive which eye is tested and bandaging of the untested eye can be avoided, reducing the overall test time and eliminating the patient's discomfort. The orders of presentation (right or left eye order testing as well as Humphrey or Oculus visual field test) were randomized among subjects and among eyes. We asked the participants to press the response button as soon as they perceived the moving stimulus (Fig.1D). The examiners (L.V., F.G., M.V.) supervised the fixation level of each participant using a monitor in the case of the Humphrey perimeter and commended to keep fixation in case of distraction to ensure adequate fixation in the case of Oculus VR perimetry. Peripheral kinetic visual field testing was performed with refractive correction (using either contact lenses of glasses) in both Oculus and Humphrey test to exclude the influence of presbyopia. Patient's refraction was assessed by autorefractometry, during the ophthalmological evaluation prior to the study. Each test performed with the Oculus started by seating the participant comfortably and adjusting the headset to produce the clearest image and avoid lens rim artifacts. The interpupillary distance was measured in each subject prior to the test as the distance between the center of the pupils and manually corrected within the headset displays.

All the devices must be connected to the same Wi-Fi network. Once the patient is ready to start the visual field test, the user selects the testing eye and waits for the patient's feedback. The three tested isopters were presented in decreasing order of magnitude of the stimulus (V/4e, IV/1e, and III/1e), followed by the localization of the blind spot, as described above. If the stimulus is not seen by the patient, a radius equal to zero is received and plotted on the map. The total exam duration is 10 min for both eyes.

C. Subjects

Following an explanation of the study procedures, written informed consent was obtained from all subjects. The study followed the tenets of the Declaration of Helsinki. A total of 42 eyes of 21 consecutive volunteers (5 men and 16 women) were recruited for this study. Nine of these subjects were in the age range of 20-30 years old, six in the range 31-40 years old, and six in the range 41-80 years old. Subject inclusion criteria for this study were in line with similar studies [10] as the following: i) age between 18 and 80 years old; ii) best-corrected visual acuity (BCVA) of at least 8/10; iii) spherical ametropia within ±6 diopters and cylindrical ametropia within ±2 diopters; v) motor ability and sufficient cognitive to perform both the tests. Subjects were excluded from the study if: i) suffering from strabismus, amblyopia, retinal vein/artery occlusion, ocular motility disorder, diabetic retinopathy, macular degeneration, and other neuro-ophthalmological diseases affecting the visual field; ii) found with relevant opacities of the cornea, lens, or vitreous body; iii) consuming miotic drugs which may compromise the visual field test; iv) underwent intraocular surgery; v) intraocular inflammation; vi) glaucoma.

D. Data Processing

All the results generated in this study with the Oculus Quest 2 are compared with those obtained with the gold standard Humphrey, to test and validate the Oculus-based kinetic perimetry reliability. Collected data were analyzed by the first author (RT) who was kept blinded to avoid a biased assessment of the outcome. GraphPad (La Jolla, CA, USA) Prism 9 software was used for data analysis and statistics. Statistical significance was assessed by multiple unpaired t test correcting for multiple comparisons using the Holm-Šídák method. Statistical significance was defined as $p < 0.05$. Data were tested for normality using the Kolmogorov-Smirnov test and the Shapiro–Wilk normality test. Simple linear regression was also conducted. Data presented are reported as mean ± standard deviation. Polar plots were generated with Python and were represented by mean and standard deviation to evaluate the variability across the data. Pearson's correlation test, Bland-Altman, scatter-plot, and boxplot analysis were conducted to evaluate the agreement among instruments.

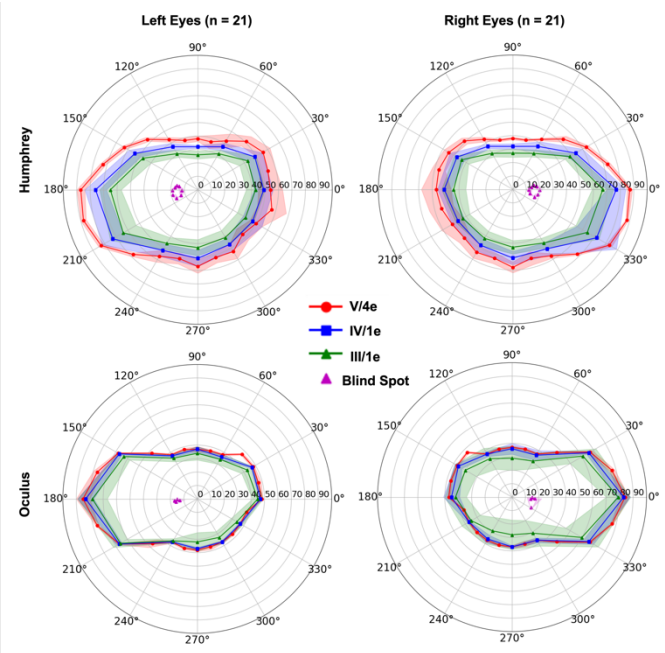

Figure 2. Kinetic visual field assessed in each eye of n = 21 individuals with Humphrey and Oculus Quest 2 headset, summarizing the isopters in polar plots. Isopters were generated with V/4e target along 24 vectors, with IV/1e and III/1e targets along 12 vectors, and finally the size of the physiological blind spot was determined. Each data point in the polar plots represents the average radius seen from the subjects involved in this study. Data are analyzed with Python (mean values ± standard deviations).

III. Results and Discussion

In this section, we present and discuss the results obtained from the comparative analysis conducted in this study. All the subjects underwent the test and did not claim any discomfort during the procedure. As kinetic perimetry presents a patient-related subjective component, we noticed that the Oculus visual field examination was well tolerated by all the patients and the decrease in the total duration time (~5 min bilaterally) compared with the Humphrey (~15 min bilaterally) was considered as an advantage by all the subjects. Patient acceptability of a new instrument is highly important since the reliability of the results is largely dependent on good patient cooperation in the case of visual field examination.

Figure 2 reports the bidimensional maps representing the sensitivity thresholds in the form of polar plots with the mean (data points) and standard deviation (shaded error bars) of each isopter tested in this study, comparing the Oculus-based kinetic perimeter with the gold standard Humphrey kinetic perimeter. It is possible to appreciate the great similarity between the two compared methodologies, as well as the interocular similarity. The Oculus perimeter showed a lower inter-variability than the Humphrey within subjects, which can be appreciated in both eyes as a decrease in the standard error. Here we tested 24 or 12 vectors for each isopter, which are sufficient numbers of vectors to obtain a boundary of equal sensitivity and produce a contour line on a topographic map.

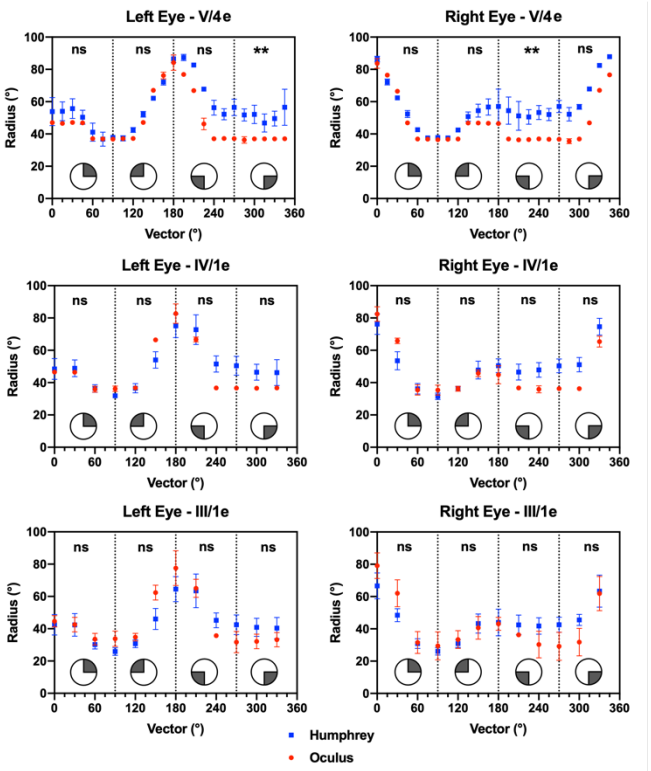

Figure 3. Comparison between visual field radius obtained with Humphrey (n = 21) and Oculus headset (n = 21) for left and right eyes using three different targets: V/4e, IV/1e, III/1e. Vector range is represented in four pie-charts to highlight differences and similarities in the four quadrants of the visual field. Data are reported as mean ± standard deviations. Statistical significance was defined as **p < 0.005.

In a normal and physiological vision, the most visible stimuli produce the largest isopters and the least visible stimuli generate the smallest isopters. For instance, since V/4e stimulus presents the greatest diameter and most intense brightness tested, it leads to a larger isopter than the smaller and dimmer IV/1e and III/1e stimuli. This mechanism is emphasized in the Humphrey visual field, while the isopters generated with the Oculus system produced a shorter gap between the three isopters. A possible explanation for this gap might be related to the external light conditions and the patient focus. In fact, even though we tested the experimental light conditions of both instruments, the Humphrey visual fields are examined in a dark environment, which does not isolate completely the patient as the Oculus headset does in VR. We estimate that the residual light in the room might create a bias in the luminance impacting the retina, which affects the visual field. This residual light, and consequently this bias, is absent in the Oculus headset since the patient is completely isolated from the external light.

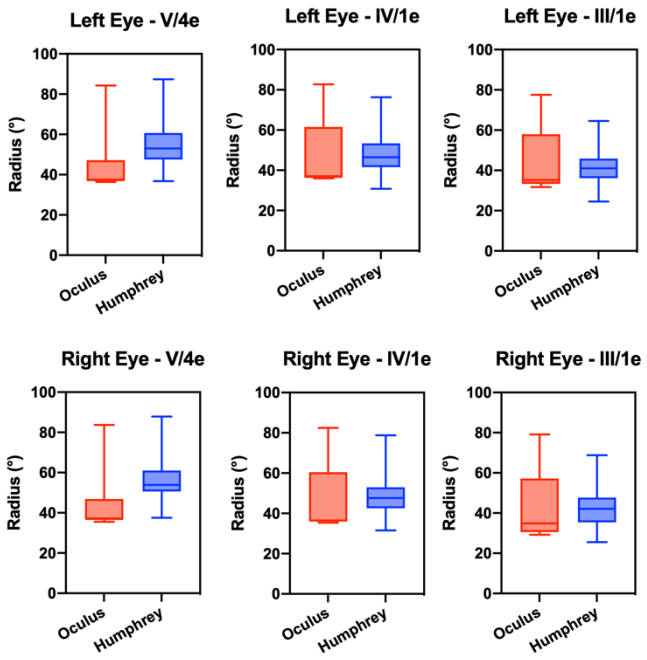

Figure 4. Boxplot comparison between visual field radius obtained with Humphrey (n = 21) and Oculus headset (n = 21) for left and right eyes using three different targets: V/4e, IV/1e, III/1e.

It has been previously reported that age influences the periphery and the center of the visual field more than the pericentric area [39], producing a linear age-related decline in threshold sensitivity due to the anatomic loss of photoreceptors, ganglion cells, and higher structures [40]. However, to date, only a few studies have been published assessing the influence of aging on visual field data, and most of these papers only consider patients with progressive diseases, such as glaucoma [41]. Therefore, to exclude any possible effect due to the patients age, we performed the statistical analysis comparing the outcomes from the two instruments by dividing the subjects into three subgroups per age range: subjects with age range 20-30 years old (n = 9), subjects with age range 31-40 years old (n = 6), and subjects with age range 41-80 years old (n = 6). No significance difference was highlighted due to the age range and results are reported in Figure S1 for the right eyes and Figure S2 for the left eyes (see Supporting Information).

Figure 3 represents the visual field radius obtained from both kinetic perimeters. In each graph, the four quadrants of the visual field are separated into temporal/nasal and superior/ inferior to highlight possible local deviances between methodologies and represented with pie charts. Significant differences between Humphrey and Oculus perimeters are highlighted only in the V/4e isopter, in the nasal inferior quadrant of the visual field for the right eye (**$p < 0.005$), and for the left eye (**$p < 0.005$). These differences, which are perfectly specular, can be explained considering the anatomic structures involved in this examination, as the visual field depends on the individual facial anatomy. In the Humphrey perimetry, the inferior visual field is physically limited by the nose. This physical limitation does not occur in the Oculus perimeter, where the nose does not represent a physical obstacle in virtual reality.

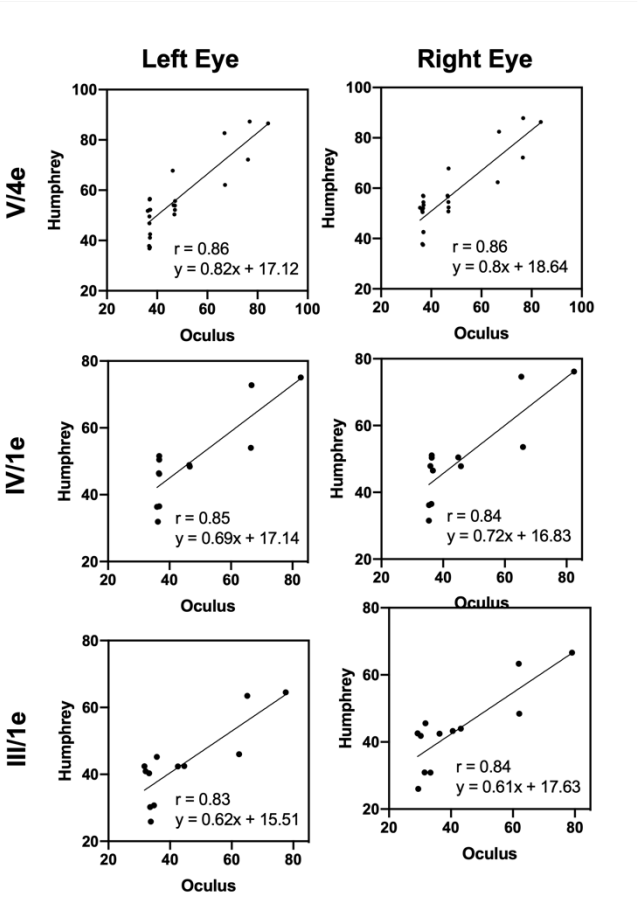

Figure 5. Scatter plots comparing visual field radius obtained with Humphrey (n = 21) and Oculus headset (n = 21) for (A) left eyes, and (B) right eyes. Correlation analysis include the Pearson r-value (r) and the slope/interception equation (***$p < 0.0005$).

Figure 4 reports boxplots and whiskers of the seen radius comparing Humphrey outcomes with those obtained with the Oculus kinetic perimeter. Boxplots present similar and comparable ranges in all the tested isopters as well as great interocular similarity. We used boxplots to complement the previously reported analysis, to assess whether a distribution was symmetric, and to identify possible outliers. Humphrey visual field presents a symmetric distribution, with the median in the middle of the box and the whiskers well-distribute on both sides. Oculus visual fields, instead, lack of symmetry since the median aligns to the bottom of the box, while the whisker is shorted on the lower end of the box, producing a distribution which is positively skewed. Median values are slightly different for the V/4e and IV/1e, while analogous median values are reported for III/1e. No outliers were found in the boxplots.

To assess whether a linear relationship exists between variables obtained with Humphrey kinetic perimetry and Oculus kinetic perimetry, we calculated the Pearson's coefficient of correlation. We found a great agreement between Oculus kinetic perimetry and Humphrey kinetic perimetry investigated in this study, with a Pearson's correlation greater than 0.83 overall (***$p < 0.0005$), indicating a strong positive correlation. In addition to the Pearson's correlation, we generated the scatter plots for each eye, and performing a linear

regression analysis, as shown in Figure 5.

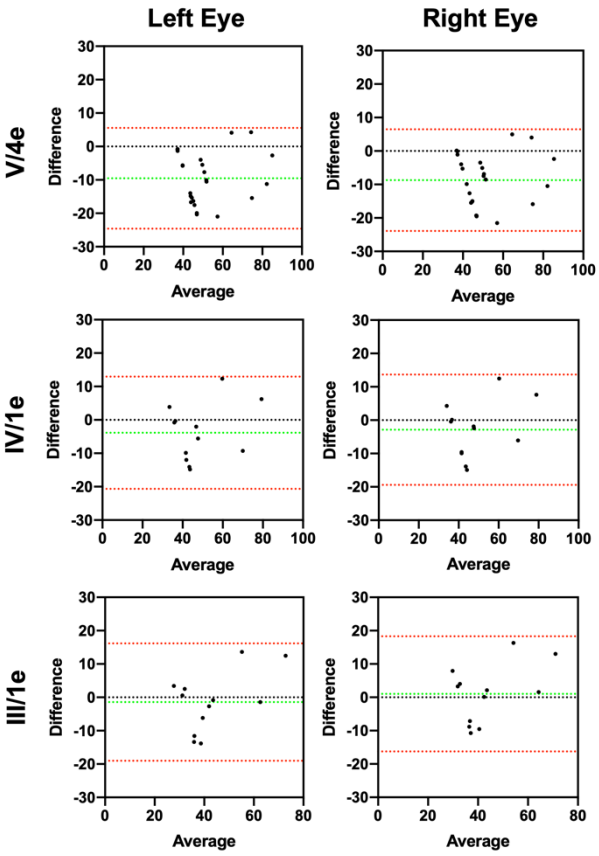

Figure 6. Bland-Altman analysis, comparing visual field radius obtained with Humphrey (n = 21) and Oculus headset (n = 21) for (A) left eyes, and (B) right eyes to evaluate the agreement among the two different instruments. In the graphs, the average of the two measurements (Oculus vs Humphrey) is plotted as the x-value, and the difference between the two measures as y-value.

Finally, the Bland-Altman analysis was conducted to evaluate the concordance between the two quantitative measurements obtained with the two instruments compared in this study and evaluating the performances of the proposed solution compared to the gold standard. Figure 6 reports the differences between the two measures on the vertical axis over the average values between the two measures over the horizontal axis. In the case of V/4e, Oculus radius produced on average lower results than the Humphrey radius, especially for the peripheral field of view (from 180° to 360°). A presence of a bias is here observed (-9.532° for the left eye, -8.722° for the right eye), while bias is neglectable in IV/1e and III/1e. The increase in the variability in IV/1e and III/1e generates reduced biases compared with the V/4e, where a significant difference is statistically reported (see Figure 3). Therefore, the biases, accuracy and limits reported in the Bland-Altman are in accordance with the other analyses reported in this study.

Statistical analysis highlighted a good agreement between the proposed solution and the standard kinetic perimetry, despite some differences in the nasal area. We believe that these differences derive from the diverse nature of the test, which excludes the nose as an obstacle to the field of view in virtual reality. The nose acts as a fixed visual reference object and the physiologic nasal visual field is smaller than the temporal visual field in the primary gaze [42]. It has been demonstrated that, regardless of the size or shape of the nose, the maximum extent of the nasal visual field was 64° when evaluated with manual Goldmann perimetry [43], [44]. For instance, in a recent study, Weber et al. [45] demonstrated that wearing a mouth-nose mask can reduce the visual field function in inferior-nasal sector of healthy subjects, especially when the nose clip was not correctly used. However, to our knowledge, no previous study involving VR perimeters discussed the nose issue. Only Wienrich et al. [46] recently demonstrated that adding a virtual nose to the VR experience can reduce simulator sickness when experiencing a VR game presented on an Oculus Rift. Future studies may focus on deepening the knowledge in this direction, comparing the kinetic perimetry on virtual reality with an additional VR element that simulates the presence of the nose, emulating the size and the shape of the patient.

This study was intended as a pilot study to investigate the feasibility of kinetic perimetry in virtual reality and comparison with gold standard kinetic perimeters. Therefore, the major limitation is the sample size (n = 42 eyes), which must be increased to gain additional knowledge and create a database with normative data for the VR kinetic perimeter. In addition, the proposed solution must be tested and validated in pathologic patients to demonstrate its diagnostic efficacy. Consequently, future studies must investigate the degree of reliability of the new instrument in detecting and quantitating visual field defects in a pathological sample.

As new devices are expected to give patients the possibility to perform visual field tests at home, relieving both patients and clinicians from in-office testing and allowing for more frequent examinations [47], our proposed solution may allow for possible application in telemedicine and patient home-monitoring since it is portable, relatively cheap, and it can be used with patients at the bedside.

IV. Conclusion

In conclusion, in this pilot study, we presented a portable automatic kinetic perimeter based on a virtual reality headset device as an innovative and alternative solution for the visual field clinical examination. We compared the performances of the new instrument with a commercially available perimeter, validating the test on 42 eyes of 21 healthy subjects. We used an Oculus Quest 2 as a VR headset, which includes a clicker for participant response feedback and an Android app designed in Unity to generate moving stimuli along vectors. Then, we determined the sensitivity thresholds by moving three different targets along 24 (V/4e) or 12 (IV/1e, III/1e) vectors from an area of non-seeing to an area of seeing and then transmitted wirelessly to a PC. The incoming kinetic results are collected and processed by a Python real-time algorithm which saves patient information into a database and displays the hill of vision in a two-dimensional map. We compared the results obtained with our Oculus kinetic perimeter with a Humphrey visual field analyzer to test reproducibility and efficacy of the proposed solution. We

obtained a good agreement between results obtained with our solution and those acquired with a commercial device, obtaining Pearson's correlation values $r > 0.83$ for each target tested. We demonstrate feasibility of VR kinetic perimetry by comparing performances between our system and a clinically used perimeter in healthy subjects, leading the way for a portable and more accessible visual field test, overcoming challenges in current kinetic perimetry practices.

V. Compliance with Ethical standards

A. Conflict of interest

All authors certify that they have no conflict of interest.

B. Ethical approval

All procedures performed in studies involving human participants were in accordance with the ethical standards of the institutional and/or national research committee and with the 1964 Helsinki Declaration and its later amendments or comparable ethical standards. In addition, this study was approved by the Polytechnic University of Turin and the School of Orthoptic at University of Turin as part of a master theses.

C. Informed consent

Informed consent was obtained from all individual participants included in the study.

D. Data availability

The data that support the findings of this study are available from the corresponding author upon reasonable request.

References

[1] C. A. Johnson, M. Wall, and H. S. Thompson, "A history of perimetry and visual field testing," *Optom Vis Sci*, vol. 88, no. 1, pp. E8-15, Jan. 2011, doi: 10.1097/OPX.0b013e3182004c3b.

[2] A. M. Mckendrick, "Recent developments in perimetry: test stimuli and procedures," *Clinical and Experimental Optometry*, vol. 88, no. 2, pp. 73–80, Mar. 2005, doi: 10.1111/j.1444-0938.2005.tb06671.x.

[3] Z. Wu and F. A. Medeiros, "Recent developments in visual field testing for glaucoma," *Curr Opin Ophthalmol*, vol. 29, no. 2, pp. 141–146, Mar. 2018, doi: 10.1097/ICU.0000000000000461.

[4] C. G. De Moraes, J. M. Liebmann, and L. A. Levin, "Detection and measurement of clinically meaningful visual field progression in clinical trials for glaucoma," *Prog Retin Eye Res*, vol. 56, pp. 107–147, Jan. 2017, doi: 10.1016/j.preteyeres.2016.10.001.

[5] D. K. Lee, M. S. Sung, and S. W. Park, "Factors Influencing Visual Field Recovery after Transsphenoidal Resection of a Pituitary Adenoma," *Korean J Ophthalmol*, vol. 32, no. 6, pp. 488–496, Dec. 2018, doi: 10.3341/kjo.2017.0094.

[6] J. H. Pula and C. A. Yuen, "Eyes and stroke: the visual aspects of cerebrovascular disease," *Stroke Vasc Neurol*, vol. 2, no. 4, Dec. 2017, doi: 10.1136/svn-2017-000079.

[7] A. Agarwal and S. Kedar, "Prognosis and Treatment of Visual Field Defects," *Semin Neurol*, vol. 35, no. 5, pp. 549–556, Oct. 2015, doi: 10.1055/s-0035-1563573.

[8] L. R. Hepworth and F. J. Rowe, "Programme choice for perimetry in neurological conditions (PoPiN): a systematic review of perimetry options and patterns of visual field loss," *BMC Ophthalmol*, vol. 18, no. 1, p. 241, Sep. 2018, doi: 10.1186/s12886-018-0912-1.

[9] E. L. Greve, "Static perimetry," *Ophthalmologica*, vol. 171, no. 1, pp. 26–38, 1975, doi: 10.1159/000307415.

[10] X. Ma, L. Tang, X. Chen, and L. Zeng, "Periphery kinetic perimetry: clinically feasible to complement central static perimetry," *BMC Ophthalmol*, vol. 21, no. 1, p. 343, Sep. 2021, doi: 10.1186/s12886-021-02056-5.

[11] G. E. Pennebaker, W. C. Stewart, J. A. Stewart, and H. H. Hunt, "The effect of stimulus duration upon the components of fluctuation in static automated perimetry," *Eye (Lond)*, vol. 6 (Pt 4), pp. 353–355, 1992, doi: 10.1038/eye.1992.72.

[12] V. Muthusamy, A. Turpin, M. J. Walland, B. N. Nguyen, and A. M. McKendrick, "Increasing the Spatial Resolution of Visual Field Tests Without Increasing Test Duration: An Evaluation of ARREST," *Translational Vision Science & Technology*, vol. 9, no. 13, p. 24, Dec. 2020, doi: 10.1167/tvst.9.13.24.

[13] S. L. Pineles *et al.*, "Automated Combined Kinetic and Static Perimetry: An Alternative to Standard Perimetry in Patients With Neuro-ophthalmic Disease and Glaucoma," *Archives of Ophthalmology*, vol. 124, no. 3, pp. 363–369, Mar. 2006, doi: 10.1001/archopht.124.3.363.

[14] R. Vonthein *et al.*, "The Normal Age-Corrected and Reaction Time–Corrected Isopter Derived by Semi-automated Kinetic Perimetry," *Ophthalmology*, vol. 114, no. 6, pp. 1065-1072.e2, Jun. 2007, doi: 10.1016/j.ophtha.2006.09.030.

[15] J. Phu, M. Kalloniatis, H. Wang, and S. K. Khuu, "Differences in Static and Kinetic Perimetry Results are Eliminated in Retinal Disease when Psychophysical Procedures are Equated," *Transl Vis Sci Technol*, vol. 7, no. 5, p. 22, Oct. 2018, doi: 10.1167/tvst.7.5.22.

[16] V. M. Mönter, D. P. Crabb, and P. H. Artes, "Reclaiming the Periphery: Automated Kinetic Perimetry for Measuring Peripheral Visual Fields in Patients With Glaucoma," *Investigative Ophthalmology & Visual Science*, vol. 58, no. 2, pp. 868–875, Feb. 2017, doi: 10.1167/iovs.16-19868.

[17] K. Nowomiejska, R. Vonthein, J. Paetzold, Z. Zagorski, R. Kardon, and U. Schiefer, "Comparison between semiautomated kinetic perimetry and conventional Goldmann manual kinetic perimetry in advanced visual field loss," *Ophthalmology*, vol. 112, no. 8, pp. 1343–1354, Aug. 2005, doi: 10.1016/j.ophtha.2004.12.047.

[18] K. Hirasawa and N. Shoji, "Learning Effect and Repeatability of Automated Kinetic Perimetry in Healthy Participants," *Current Eye Research*, vol. 39, no. 9, pp. 928–937, Sep. 2014, doi: 10.3109/02713683.2014.888450.

[19] A. Chandrinos and D.-D. Tzamouranis, "A Review of Learning Effect in Perimetry," *Ophthalmology Research: An International Journal*, pp. 23–30, Apr. 2020, doi: 10.9734/or/2020/v12i230144.

[20] F. J. Rowe, L. R. Hepworth, K. L. Hanna, M. Mistry, and C. P. Noonan, "Accuracy of kinetic perimetry assessment with the Humphrey 850; an exploratory comparative study," *Eye (Lond)*, vol. 33, no. 12, pp. 1952–1960, Dec. 2019, doi: 10.1038/s41433-019-0520-1.

[21] S. Wilscher, B. Wabbels, and B. Lorenz, "Feasibility and outcome of automated kinetic perimetry in children," *Graefes Arch Clin Exp Ophthalmol*, vol. 248, no. 10, pp. 1493–1500, Oct. 2010, doi: 10.1007/s00417-010-1342-9.

[22] S. Hashimoto, C. Matsumoto, M. Eura, S. Okuyama, and Y. Shimomura, "Evaluation of kinetic programs in various automated perimeters," *Jpn J Ophthalmol*, vol. 61, no. 4, pp. 299–306, Jul. 2017, doi: 10.1007/s10384-017-0516-y.

[23] C. D. Riemann, S. Hanson, and J. A. Foster, "A comparison of manual kinetic and automated static perimetry in obtaining ptosis fields," *Arch Ophthalmol*, vol. 118, no. 1, pp. 65–69, Jan. 2000, doi: 10.1001/archopht.118.1.65.

[24] T. S. Prata, C. G. V. D. Moraes, F. N. Kanadani, R. Ritch, and A. Paranhos, "Posture-induced Intraocular Pressure Changes: Considerations Regarding Body Position in Glaucoma Patients," *Survey of Ophthalmology*, vol. 55, no. 5, pp. 445–453, Sep. 2010, doi: 10.1016/j.survophthal.2009.12.002.

[25] F. B. Daga, A. Diniz-Filho, E. R. Boer, C. P. B. Gracitelli, R. Y. Abe, and F. A. Medeiros, "Fear of falling and postural reactivity in patients with glaucoma," *PLoS One*, vol. 12, no. 12, p. e0187220, 2017, doi: 10.1371/journal.pone.0187220.

[26] M. Montelongo, A. Gonzalez, F. Morgenstern, S. P. Donahue, and S. L. Groth, "A Virtual Reality-Based Automated Perimeter, Device, and Pilot Study," *Transl Vis Sci Technol*, vol. 10, no. 3, p. 20, Mar. 2021, doi: 10.1167/tvst.10.3.20.

[27] R. L. Z. Goh, Y. X. G. Kong, C. McAlinden, J. Liu, J. G. Crowston, and S. E. Skalicky, "Objective Assessment of Activity Limitation in Glaucoma with Smartphone Virtual Reality Goggles: A Pilot Study," *Transl Vis Sci Technol*, vol. 7, no. 1, p. 10, Jan. 2018, doi: 10.1167/tvst.7.1.10.

[28] R. Terracciano, A. Sanginario, S. Barbero, D. Putignano, L. Canavese, and D. Demarchi, "Pattern-Reversal Visual Evoked Potential on Smart Glasses," *IEEE J Biomed Health Inform*, vol. 24, no. 1, pp. 226–234, Jan. 2020, doi: 10.1109/JBHI.2019.2899774.

[29] R. Terracciano, A. Sanginario, L. Puleo, and D. Demarchi, "A novel system for measuring visual potentials evoked by passive head-mounted display stimulators," *Doc Ophthalmol*, vol. 144, no. 2, pp. 125–135, Apr. 2022, doi: 10.1007/s10633-021-09856-6.

[30] D. Wroblewski, B. A. Francis, A. Sadun, G. Vakili, and V. Chopra, "Testing of visual field with virtual reality goggles in manual and visual grasp modes," *Biomed Res Int*, vol. 2014, p. 206082, 2014, doi: 10.1155/2014/206082.

[31] T. M. Aslam *et al.*, "Diagnostic Performance and Repeatability of a Novel Game-Based Visual Field Test for Children," *Invest Ophthalmol Vis Sci*, vol. 59, no. 3, pp. 1532–1537, Mar. 2018, doi: 10.1167/iovs.17-23546.

[32] S. Tsapakis *et al.*, "Visual field examination method using virtual reality glasses compared with the Humphrey perimeter," *Clin Ophthalmol*, vol. 11, pp. 1431–1443, 2017, doi: 10.2147/OPTH.S131160.

[33] S. Tsapakis *et al.*, "Home-based visual field test for glaucoma screening comparison with Humphrey perimeter," *Clin Ophthalmol*, vol. 12, pp. 2597–2606, Dec. 2018, doi: 10.2147/OPTH.S187832.

[34] P. Narang, A. Agarwal, M. Srinivasan, and A. Agarwal, "Advanced Vision Analyzer–Virtual Reality Perimeter: Device Validation, Functional Correlation and Comparison with Humphrey Field Analyzer," *Ophthalmology Science*, vol. 1, no. 2, p. 100035, Jun. 2021, doi: 10.1016/j.xops.2021.100035.

[35] T. Kimura, C. Matsumoto, and H. Nomoto, "Comparison of head-mounted perimeter (imo®) and Humphrey Field Analyzer," *Clin Ophthalmol*, vol. 13, pp. 501–513, Mar. 2019, doi: 10.2147/OPTH.S190995.

[36] C. Matsumoto *et al.*, "Visual Field Testing with Head-Mounted Perimeter 'imo,'" *PLOS ONE*, vol. 11, no. 8, p. e0161974, ago 2016, doi: 10.1371/journal.pone.0161974.

[37] P. Kunumpol *et al.*, "GlauCUTU: Virtual Reality Visual Field Test," *Annu Int Conf IEEE Eng Med Biol Soc*, vol. 2021, pp. 7416–7421, Nov. 2021, doi: 10.1109/EMBC46164.2021.9629827.

[38] S. L. Groth, "New Strategies for Automated Perimetry: Historical Perspective and Future Innovations," *J Curr Glaucoma Pract*, vol. 15, no. 3, pp. 103–105, 2021, doi: 10.5005/jp-journals-10078-1321.

[39] A. Haas, J. Flammer, and U. Schneider, "Influence of age on the visual fields of normal subjects," *Am J Ophthalmol*, vol. 101, no. 2, pp. 199–203, Feb. 1986, doi: 10.1016/0002-9394(86)90595-7.

[40] G. J. Jaffe, J. A. Alvarado, and R. P. Juster, "Age-Related Changes of the Normal Visual Field," *Archives of Ophthalmology*, vol. 104, no. 7, pp. 1021–1025, Jul. 1986, doi: 10.1001/archopht.1986.01050190079043.

[41] P. Brusini, "Ageing and visual field data," *Br J Ophthalmol*, vol. 91, no. 10, pp. 1257–1258, Oct. 2007, doi: 10.1136/bjo.2007.117978.

[42] W. H. Swanson, M. W. Dul, D. G. Horner, and V. E. Malinovsky, "Individual differences in the shape of the nasal visual field," *Vision Research*, vol. 141, pp. 23–29, Dec. 2017, doi: 10.1016/j.visres.2016.04.001.

[43] J. S. Glaser, "The Nasal Visual Field," *Archives of Ophthalmology*, vol. 77, no. 3, pp. 358–360, Mar. 1967, doi: 10.1001/archopht.1967.00980020360013.

[44] S. G. Schwartz, C. T. Leffler, P. S. Chavis, F. Khan, D. Bermudez, and H. W. Flynn, "The Monocular Duke of Urbino," *Ophthalmol Eye Dis*, vol. 8, no. Suppl 1, pp. 15–19, 2016, doi: 10.4137/OED.S40918.

[45] A. Weber, B. Hohberger, and A. Bergua, "Mouth-nose masks impair the visual field of healthy eyes," *PLOS ONE*, vol. 16, no. 5, p. e0251201, mag 2021, doi: 10.1371/journal.pone.0251201.

[46] C. Wienrich, C. K. Weidner, C. Schatto, D. Obremski, and J. H. Israel, "A Virtual Nose as a Rest-Frame - The Impact on Simulator Sickness and Game Experience," in *2018 10th International Conference on Virtual Worlds and Games for Serious Applications (VS-Games)*, Sep. 2018, pp. 1–8. doi: 10.1109/VS-Games.2018.8493408.

[47] A. S. Camp and R. N. Weinreb, "Will Perimetry Be Performed to Monitor Glaucoma in 2025?," *Ophthalmology*, vol. 124, no. 12S, pp. S71–S75, Dec. 2017, doi: 10.1016/j.ophtha.2017.04.009.